



REGULAR ARTICLE

Microwave Absorption Properties of a Composite Material Based on Polyvinyl Chloride and Yttrium Iron Garnet

L.M. Grishchenko¹, D.O. Zhytnyk², M.O. Popov², H.L. Chumak², V.Yu. Malyshev², I.V. Fesych²,
Y.V. Noskov³, A.I. Ivanisik², I.P. Matushko^{2,*}

¹ Chuiko Institute of Surface Chemistry, National Academy of Science of Ukraine, 03164 Kyiv, Ukraine

² Taras Shevchenko National University of Kyiv, 01601 Kyiv, Ukraine

³ Kukhar Institute of Bioorganic Chemistry and Petrochemistry, National Academy of Science of Ukraine, 02160 Kyiv, Ukraine

(Received 15 May 2025; revised manuscript received 23 August 2025; published online 29 August 2025)

This study reports the fabrication of the flexible polyvinyl chloride composite films embedded with yttrium iron garnet and analysis of their microwave properties. The films with 0.25 mm thickness were created using temperature pressing at 175°C and 10 MPa, with yttrium iron garnet filler concentrations ranging from 0.2 to 30 wt % and dibutyl phthalate used as a plasticizer. Both the ferrite powder and manufactured films were characterized using SEM, TGA, PXRD, and FTIR. SEM analysis showed that the $\text{Y}_3\text{Fe}_5\text{O}_{12}$ ferrite powder consists of agglomerated, near-spherical crystallites. EDX analysis confirmed the presence of only yttrium, iron, and oxygen, indicating high purity of the sample. Thermogravimetric analysis demonstrated high thermal stability of $\text{Y}_3\text{Fe}_5\text{O}_{12}$ ferrite, mass loss was only 1.42 % when heated from 25 to 900 °C. According to the diffraction experiment, it was found that the studied sample is single-phase and has a high degree of crystallinity. From the IR spectrum of yttrium ferrite $\text{Y}_3\text{Fe}_5\text{O}_{12}$, it was found that in the range of 550-680 cm^{-1} , three intense absorption bands are observed at 566 cm^{-1} , 610 cm^{-1} , and 656 cm^{-1} , which are characteristic of asymmetric stretching vibrations of Fe-O of the tetrahedral group FeO_4 . Analysis of the films spectra shows the presence of PVC and ferrite due to their distinct characteristic spectral bands. It has been found that the presence of ferrite in the composite can cause a shift in the position of some characteristic polymer bands. Microwave measurements revealed very low transmission losses, – (0.1-0.3) dB and negligible reflection. Reflection losses were in the range from – 19.3 to – 23.7 dB, exhibiting an irregular variation with ferrite concentration: losses initially increased with increasing ferrite content, then decreased, and subsequently increased again.

Keywords: Yttrium iron garnet, Polyvinyl chloride, Composite material, Microwave losses, Electromagnetic shielding, Microwave absorbing materials.

DOI: [10.21272/jnep.17\(4\).04037](https://doi.org/10.21272/jnep.17(4).04037)

PACS numbers: 41.20.Jb, 77.22.Gm, 82.35.Np

1. INTRODUCTION

Ferrites are commonly used magnetic materials for radio electronics, radio engineering, automation, computer engineering etc. [1, 2]. They are utilized both as bulk components and as a part of nanocomposite functional materials. Other notable ferrite application areas include high-pressure monitoring electronic devices and microchip high-speed computing systems with ultra-low switching energy [3]. Rare-earth ferrites with the garnet crystallographic structure attract researcher's interest due to their outstanding magnetic and electric properties and perspectives for applications in magnetooptical systems, magnetic cooling etc [4, 5]. Among them the most extensively investigated is yttrium iron garnet (YIG), with chemical formula $\text{Y}_3\text{Fe}_5\text{O}_{12}$, which has a cubic crystal structure (eight formula units per unit cell) and belongs to the space group $\text{Ia}\bar{3}\text{d}$ [6]. In each unit cell Y^{3+} atoms occupy the 24 dodecahedral c-sites and Fe^{3+} atoms occupy both the 16 octahedral a-sites and the 24 tetragonal d-sites, which are formed by

the surrounding O^{2-} ions [7]. The essential magnetic characteristics of YIG come from the specific orientation of the magnetic moments of ferric ions. Namely, the spins of octahedrally positioned Fe^{3+} ions are oriented antiparallel to those of tetrahedrally positioned ions (nonmagnetic Y^{3+} ions located in the dodecahedral site do not contribute to the net magnetic moment). This orientation of magnetic moments in octahedral and tetrahedral sublattices is due to the superexchange inter-atom interaction between Fe^{3+} ions mediated by the nearby oxygen atoms [8]. Hence the effective magnetic moment of one formula unit of YIG essentially equals to magnetic moment of one Fe^{3+} ion, which is 5 Bohr magnetons.

YIG belongs to a class of magnetic oxides with a broad range of important practical applications, due to its magnetic, mechanical and chemical properties, such as high melting point, high Curie temperature, great thermal stability, excellent chemical stability, thermal conductivity, very large resistivity, and low thermal expansion. In view of its diverse properties, YIG nano-

* Correspondence e-mail: mipigor@gmail.com



particles (NPs) are the best suitable materials for a wide variety of applications in microwave and magneto-optic communication devices due to its extremely low microwave magnetic losses and large specific Faraday rotation in near infrared range (for Bi-doped YIG) [9, 10]. In particular, both bulk ferrite specimens and ferrite-containing polymer composites are utilized in such microwave devices as filters, isolators and circulators [11, 12]. YIG, among other ferrites, is also considered for applications in composite materials designed for microwave absorption and reflection control [13-16]. Those composite materials usually include magnetic particles, metallic particles, and electrically conductive carbon (nano)materials, all being encapsulated in dielectric polymer matrix [17-19]. Such protective coating makes it difficult for the radar to detect shielded objects by absorbing most of the electromagnetic wave energy sent by the radar. Also, radio absorbing materials are used to protect the object located behind them from electromagnetic irradiation, in which case it is also necessary to ensure maximum absorption of electromagnetic wave in a composite material in a specified frequency band.

The advantages of using ferrite material as a part of radio absorber materials are numerous. Firstly, magnetic fillers in the composite increase the effective permeability μ of the material thus essentially reducing the reflectivity of a composite. Indeed, the minimum reflection of incident electromagnetic wave into environment would occur is the effective permittivity ε and permeability μ of medium are equal to or at least close to each other. Since composite absorber usually have $\varepsilon > 1$, one needs to increase μ in order to "balance" the dielectric permittivity and inclusion of magnetic particles just works in that way. Secondly, introduction of magnetic constituents decreases the electrical thickness of the coating (which is inversely proportional to $\sqrt{\varepsilon\mu}$). As a result, the same reflection characteristics may be achieved for lower thickness of absorber coating (reducing the weight and price of absorbing coating). Finally, ferrite particles demonstrate increased selective absorption of electromagnetic energy in the frequency regions of magnetic moments precession. This phenomenon can occur both when some external magnetic field is applied to the material (then it is called ferromagnetic resonance) and in the zero external magnetic field (in which case it is referred to as natural ferromagnetic resonance). The natural ferromagnetic resonance, among others, includes the domain walls oscillation effect. Naturally, this additional magnetic absorption increases the overall microwave losses and improves the characteristics of absorber. However the actual frequency and bandwidth of (natural) ferromagnetic resonance strongly depend on ferrite chemical composition, nanoparticles shape and dimensions, temperature and magnitude and orientation of external magnetic field (if any). Thus, it is necessarily to investigate the reflection/transmission properties of composite material not at some specific frequency, but in a frequency band as broad as possible. That will allow one to pinpoint any possible peculiarities in material's microwave behavior, whether due to a ferromagnetic resonance or some other potentially useful phenomenon.

In spite of the perspectives of ferrite-based absorbers, only a few researches on such multi-component systems are published in scientific literature. Specifically, the structural and microwave properties of two-component ferrite-polymer composite system in wide range of ferrite filler concentrations are investigated insufficiently.

The purpose of this research was to obtain the two-component ferrite-polymer systems based on polyvinyl chloride and iron-yttrium garnet with a wide range of the garnet concentrations (0.2-30 % by mass), to investigate its physical and chemical properties and to study the effect of ferrite concentration on the microwave properties of the obtained composite material in the broad microwave frequency range and determine the perspectives of such material application for radio absorbing coatings.

2. DESCRIPTION OF OBJECTS AND INVESTIGATION METHODS

An industrial sample of ferrite was used as the initial sample. PVC was purchased from Sigma-Aldrich. Before introduction into PVC, ferrite was crushed using ball mills. Production of PVC/ferrite films was carried out as follows: first, ferrite powder was ground in a mortar, then 0.2 g of PVC powder was mixed with the required amount of ferrite. The resulting mixture was ground in an agate mortar to a homogeneous state, placed in a mold on a polyamide substrate, and 70 mg of plasticizer (dibutyl phthalate) was added. Then it was pressed at 175 °C and a pressure of 10 MPa with a 1-minute holding time.

Thermogravimetry and Differential Thermal (TG/DTA) Analysis

Thermal gravimetric analysis (TGA) was performed using a Q-1500 D derivatograph of the system of F. Paulik, J. Paulik, and L. Erdey and a DTG-60H analyzer (Shimadzu, Japan) at a heating rate of 10 °C/min from room temperature to 800 °C [18, 19]. 1-2 mg of powdered sample was placed into alumina crucibles. The experiments were performed in air atmosphere at a flow rate of 100 mL/min, with pure α -Al₂O₃ used as a reference substance.

Scanning Electron Microscopy

The surface morphology of ferrite was observed by scanning electron microscopy (SEM) on a Tescan Mira 3 LMU microscope [20-22].

Fourier Transform Infrared Spectroscopy (FTIR)

Infrared spectra of the ground ferrite powder were obtained in the transmission mode in the range of 400-4000 cm⁻¹ using a Fourier transform infrared spectrophotometer Spectrum BX FT-IR (Perkin Elmer, USA). A portion of the studied powder was mixed with high-purity KBr at a 1:100 weight ratio and pressed into translucent tablets. IR spectra were recorded with a resolution of 2 cm⁻¹ and a signal accumulation of 32 scans.

Fourier transform infrared (FTIR) spectra of the films were recorded on a Nicolet iS50 FTIR spectrometer [18, 19].

Powder X-Ray Diffraction (PXRD)

Phase composition and crystal structure were studied by powder X-ray diffraction (PXRD) with a Shimadzu LabX XRD-6000 diffractometer at room temperature. The diffraction data were collected in the Bragg-Brentano geometry using Cu K α radiation ($\lambda_{\text{Cu}} = 1.54056 \text{ \AA}$) operating at 35 kV and 30 mA. The XRD pattern was recorded in an angle range $2\theta = 5\text{--}70^\circ$ with a 0.02° step range and a scanning speed of $1.2^\circ \text{ min}^{-1}$. The observed XRD profile was fitted with the pseudo-Voigt peak profile function using Rietveld analysis on FullProf Suite software (version July 2017). The starting crystal structure refinement parameters were taken from the $\text{Y}_3\text{Fe}_5\text{O}_{12}$ garnet-type structure (COD Card Number 96-210-1365). The average crystallite size (DW-H) and lattice strain (ε) were calculated from Williamson-Hall plot.

The average crystallite size ($D_{\text{W-H}}$) and lattice strain ε of $\text{Y}_3\text{Fe}_5\text{O}_{12}$ were determined from the full-width at half-maximum (FWHM) of peaks with different diffraction angles 2θ by employing the Williamson-Hall method using formula

$$\beta_{hkl} \cos \theta_{hkl} = K \cdot \lambda / D_{\text{W-H}} + 4\varepsilon \sin \theta_{hkl} \quad (1)$$

where β_{hkl} is the FWHM (in radians) of diffraction reflexes with Miller indices (hkl), $D_{\text{W-H}}$ is the crystallite size and K is a proportionality constant related to the shape factor of the crystallite (for spherical-shaped crystallites with cubic structure this value is approximately 0.89), λ is the X-ray radiation wavelength (for Cu-anode X-ray source $\lambda = 1.5406 \text{ \AA}$), and θ_{hkl} is the diffraction angle (in radians).

Calculation of the X-ray density D_X of the samples was carried out according to the formula:

$$D_X = Z \cdot M_r / (V \cdot N_A), \quad (2)$$

where Z is the number of formula units per unit cell; M_r is the molecular weight of ferrite (in $\text{g} \cdot \text{mol}^{-1}$); V is the unit cell volume in cm^3 ; N_A is the Avogadro's number ($6.022 \cdot 10^{23} \text{ mol}^{-1}$).

Based on the results of the X-ray diffraction experiment, the dislocation density δ can also be calculated, which is defined as the length of dislocation lines per unit volume of the sample and is calculated by the formula:

$$\delta = 1/(D_{\text{W-H}})^2 \quad (3)$$

Using $D_{\text{W-H}}$ obtained from Williamson-Hall method we calculated dislocation density value about $15 \cdot 10^{13} \text{ line/m}^2$.

Microwave Properties Measurements

The high-frequency microwave reflection losses (S_{11}) and transmission microwave losses (S_{21}) of prepared composite materials were measured with a scalar network analyzer in the X-band (8-12 GHz) using the standard metal rectangular waveguide. The network analyzer measures the absolute values (modules) of microwave scattering parameters (S-parameters) of various microwave devices, components and samples in logarithmic scale. They are defined as following:

$$S_{21} = 10 \lg \left(\frac{P_T}{P_I} \right) = 10 \lg \left(\frac{E_T^2}{E_I^2} \right) \quad (4)$$

$$S_{11} = 10 \lg \left(\frac{P_R}{P_I} \right) = 10 \lg \left(\frac{E_R^2}{E_I^2} \right)$$

where P_I is the initial (incident) electromagnetic wave power, P_T is the power transmitted through the sample and P_R is the reflected power (see Fig. 1). Correspondently, the E_I , E_T , and E_R are the electric field strengths of the incident, transmitted and reflected waves. Those quantities have a straightforward physical interpretation: S_{11} quantify the portion of electromagnetic energy reflected from the sample under investigation and S_{21} shows the portion of energy that is transmitted through it. From this data the electromagnetic wave absorption coefficient A (in relative units) may be deduced using the power balance equation

$$A = 1 - 10^{S_{11}/10} - 10^{S_{21}/10} \quad (5)$$

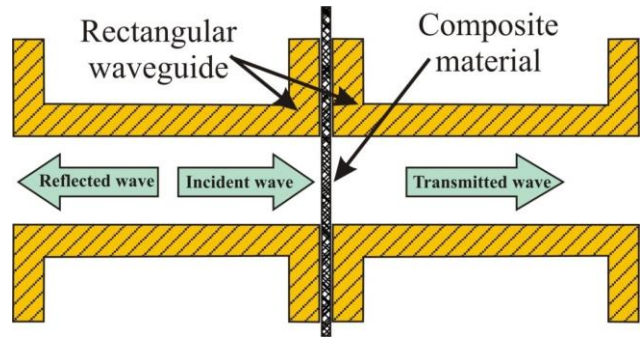


Fig. 1 – Experimental setup for X-band microwave spectroscopy measurements

During the measurements the polyvinyl chloride-ferrite composite specimens were sandwiched between the flanges of the waveguide, thus the specimen's plane was oriented perpendicularly to the propagation vector of waveguide's H_{10} electromagnetic mode. The area of the samples was large enough to completely fill the cross-section of the waveguide (see Fig. 1 for details).

3. RESULTS AND DISCUSSION

SEM and SEM-EDX

Figures 2 a,b show that the $\text{Y}_3\text{Fe}_5\text{O}_{12}$ ferrite powder consists of agglomerated, near-spherical crystallites. This agglomeration is likely due to magnetic interactions between the nanoparticles. EDX analysis (Fig. 2c) confirmed the presence of only yttrium, iron, and oxygen, indicating high purity of the sample. The Y/Fe atomic ratios obtained from EDX closely match the expected composition, confirming the homogeneity of the ferrite surface and nominal composition of the garnet.

Thermogravimetric Analysis of $\text{Y}_3\text{Fe}_5\text{O}_{12}$ Ferrite

A thermogravimetric analysis demonstrates the high thermal stability of $\text{Y}_3\text{Fe}_5\text{O}_{12}$ ferrite. The sample exhibited a mass loss of only 1.42 % when heated from 25 to 900 $^\circ\text{C}$, consistent with previous studies [23] that show structural stability up to 1200 $^\circ\text{C}$. The consistent

mass observed throughout the high temperature range supports the hypothesis that the ferrite's structure contains exclusively Fe^{3+} ions in both tetrahedral and octahedral positions.

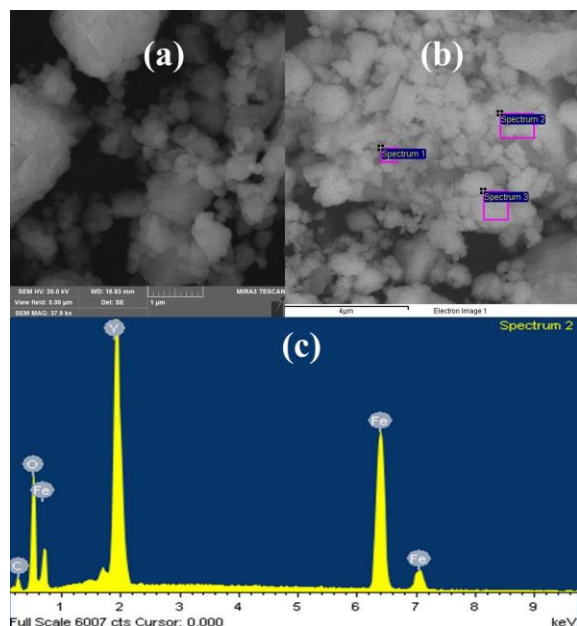


Fig. 2 – (a, b) SEM micrographs of the $\text{Y}_3\text{Fe}_5\text{O}_{12}$ ferrite and (c) EDX spectrum taken from (b)

Phase Analysis and Structure Characterization of $\text{Y}_3\text{Fe}_5\text{O}_{12}$ Ferrite

The powder X-Ray diffraction pattern of commercial ferrite is shown in Figs. 3, 4.

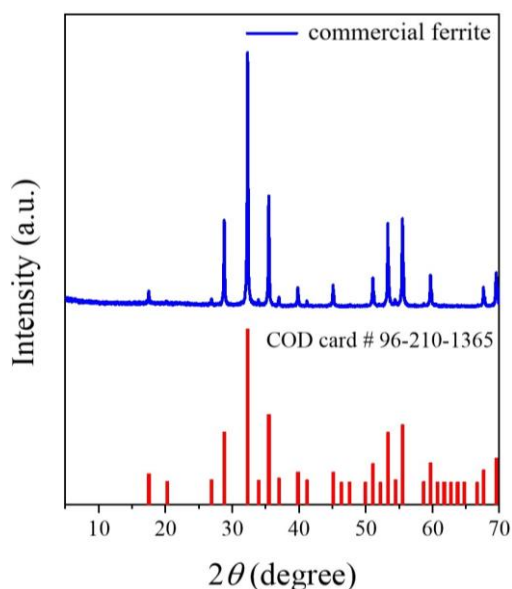


Fig. 3 – Comparison of the experimental diffractogram of ferrite powder ground in a ball mill and a standard sample from the powder diffraction data base (red lines, COD card No. 96-210-1365)

According to the data of the diffraction experiment, it was established that the studied sample is single-phase. The positions and intensities of the reflexes in the experimental diffractogram completely coincide with the cor-

responding peaks for the theoretically calculated diffraction pattern of pure yttrium ferrogarnet of the composition $\text{Y}_3\text{Fe}_5\text{O}_{12}$ (COD card number № 96-210-1365). All reflections in the diffractogram are indexed in cubic syn-gony with the space group $\text{Ia}\bar{3}\text{d}$. The refined values of the crystal lattice parameter $a = b = c = 12.375 \pm 0.001 \text{ \AA}$, the unit cell volume $V = 1895.12 \pm 0.03 \text{ \AA}^3$ and the calculated theoretical density $\rho_{\text{XRD}} = 5.173 \text{ g/cm}^3$ agree well with the literature data [24, 25].

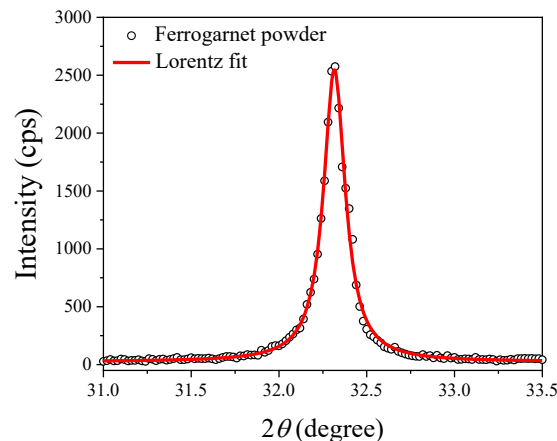


Fig. 4 – Fitting a most intense Bragg peak with Miller indices (420) of ferrite powder using Lorentz function

Size of Coherent Scattering Regions

As can be seen from the data in Table 1, the value of the D_{420} scattering crystallite size for a pre-crushed commercial ferrite sample is approximately $192 \pm 8 \text{ nm}$. Thus, the powder X-ray diffraction data confirm the presence of submicron particles in the ferrite composition. And the dislocation density δ , which is calculated as $\delta = (D_{420})^{-2}$, is equal to $3 \cdot 10^{-5} \text{ nm}^{-2}$. The dislocation density quantitatively determines the crystallinity of the sample, and its small value indicates a high degree of crystallinity of the studied ferrite.

Table 1 – Experimental parameters of the Scherrer formula, using which the size of the D_{420} coherent scattering regions in the ferrogarnet phase was determined

Sample	2θ , degree	β , radian	$\cos \theta$	λ , nm	K	D_{420} , nm
Ferrite powder	32.315	0.0008	0.961	0.154	0.9	192

IR Spectroscopic Studies on Polycrystalline $\text{Y}_3\text{Fe}_5\text{O}_{12}$ Ferrite

To study the optical properties of $\text{Y}_3\text{Fe}_5\text{O}_{12}$, spectroscopic measurements were performed in the IR and near-IR regions.

Fig. 5 shows the IR spectrum of yttrium ferrite $\text{Y}_3\text{Fe}_5\text{O}_{12}$ with garnet structure. As can be seen from the transmission spectrum in the range of $550\text{--}680 \text{ cm}^{-1}$, three intense absorption bands are observed at 566 cm^{-1} , 610 cm^{-1} and 656 cm^{-1} , which are characteristic of the asymmetric stretching vibrations of Fe-O of the tetrahedral group FeO_4 . No bands in the region of $3200\text{--}3600 \text{ cm}^{-1}$ and at 1680 cm^{-1} , which correspond to the stretching vibrations of the O-H bond and the deformation vibrations of H-O-H,

were detected, which indicates the absence of adsorbed water molecules on the surface of the commercial ferrite powder and confirms the results of thermogravimetric analysis. For the garnet structure, the vibrations of the Fe-O bond in the octahedral oxygen environment cannot be recorded, since they are detected at wave numbers of $300\text{--}400\text{ cm}^{-1}$ and are outside the measured spectral interval.

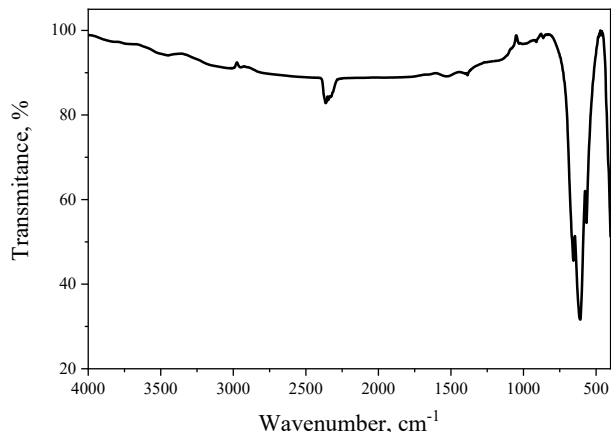


Fig. 5 – IR spectra of yttrium ferrogarnet $\text{Y}_3\text{Fe}_5\text{O}_{12}$

Fig. 6 shows the FTIR spectra of a series of PVC films with different ferrite content.

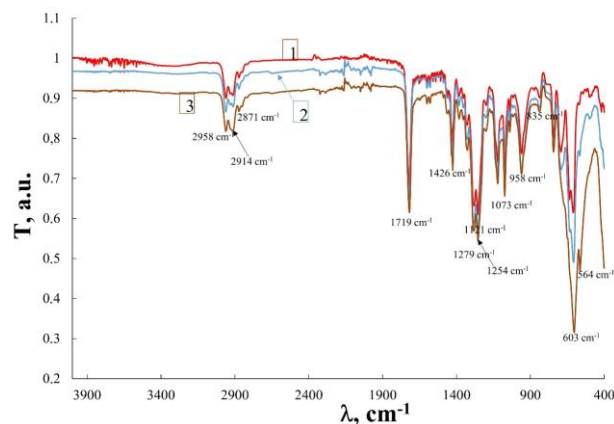


Fig. 6 – FTIR spectra of PVC films filled with different amounts of ferrite: 1) 0 % of ferrite (pure PVC), 2) 5 % of ferrite, 3) 30 % of ferrite

The analysis of the spectra reveals the presence of PVC and ferrite through their distinct spectral bands. The short-wavelength region indicates ferrite's presence, which also seems to subtly alter PVC's typical band positions. Specific PVC bands are identified: 2914 cm^{-1} (elastic vibrations in PVC macromolecules [21]), 1719 cm^{-1} (carbonyl C=O in polymer molecules, indicating PVC oxidation [21]), 1426 cm^{-1} (CH_2 deformation vibrations [21]), the doublet band with a maximum at $1254\text{--}1279\text{ cm}^{-1}$ (CH-Cl out-of-plane angular deformation [21]), 958 cm^{-1} (C-H out-of-plane trans-deformation [21]), and 835 , 603 , and 690 cm^{-1} (elastic vibrations of the C-Cl bond [21]). Bands at 1073 , 1121 , 2871 , and 2958 cm^{-1} signal the presence of the plasticizer, DBP [21]. While ferrite bands are mostly obscured by PVC's strong signals, a noticeable broad peak at 564 cm^{-1} , more

prominent in high-ferrite content samples, suggests a metal-oxygen bond [21]. Finally, a faint, broad band around 3400 cm^{-1} points to the presence of hydroxyl groups.

Microwave Properties Measurements

The summary of the microwave measurements is presented in Fig. 7. All the measured samples demonstrate very low transmission losses and nearly negligible reflection (see Table 2 for numerical details). The magnitude of the transmission losses through the studied composites in the given frequency range are within $-(0.1\text{--}0.4)\text{ dB}$ (see Fig. 7b) and, since the reflection is very low, those losses should be attributed not to the impedance mismatch between sample and waveguide, but to the electromagnetic wave attenuation inside the composite material. Consequently, an almost lossless transmission implies that the intrinsic dielectric and magnetic absorption in the studied composite material is low. Regarding the behavior of the PVC/YIG compositions with different amount of ferrite filler we observe the unambiguous trend of increased transmission losses with the rise of ferrite component mass fraction. That can be explained by increment of net magnetic losses of material (characterized by the imaginary part of high-frequency magnetic permeability μ'') due to increased proportion of ferrite constituent.

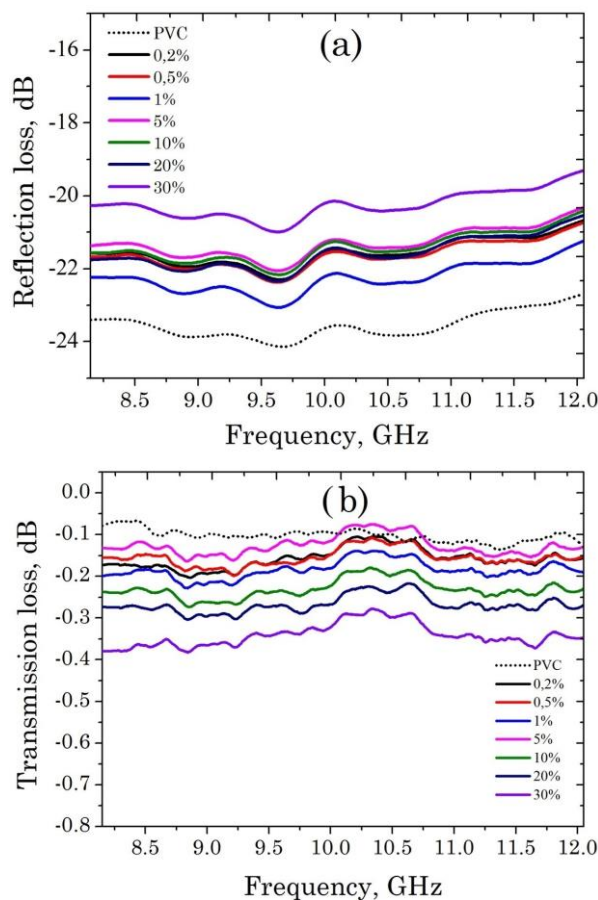


Fig. 7 – Reflection a) and transmission b) losses of the two-component polyvinyl chloride/iron-yttrium garnet thin composite layers with 0.2–30 % garnet concentrations measured in the 8–12 GHz frequency range

However, it is known that ferrite materials demonstrate the largest increase of electromagnetic wave absorption at frequencies near to their ferromagnetic resonance frequency (at the presence of external bias magnetic field). If the magnetic field is absent only a so-called natural ferromagnetic resonance may take place. This phenomenon in ferrite materials with garnet structure (like YIG) usually is registered at frequencies below than few GHz, therefore its effect on internal losses for electromagnetic waves with frequencies so much different from natural FMR frequency as X-band should be insignificant. And that is exactly what was measured: whereas composite material's internal losses do grow with ferrite concentration, this growth is rather small in absolute magnitude. The small absolute value of transmission losses can be attributed to a rather small thickness of the investigated material (0.25 mm). Should the composite sample be prepared with a more suitable for radio absorption coatings thickness of 3-5 mm, the much larger transmission losses are expected.

The reflection losses (Fig. 7a) for composites of all compositions are within $-(19.3-23.7)$ dB range and demonstrate rather irregular behavior with YIG concentration: when ferrite amount grows, the average losses first increase then decrease then increase again (see Table 2). We assume that this is a result of nonlinear variation of impedance mismatch between composite film and waveguide which is then transformed into variations of reflectivity. Indeed, the reflection losses can be calculated as

$$S_{11} = 20 \lg \left(\frac{Z_0 - Z_S}{Z_0 + Z_S} \right) \quad (6)$$

where Z_0 is the impedance of empty waveguide and Z_S is the impedance of waveguide's section filled with PVC/YIG sample. Whereas Z_0 is fixed, the Z_S will strongly depend on both, dielectric and magnetic parameters of the material. In our case the ferrite filler has larger dielectric constant ε and larger magnetic permeability μ than PVC matrix. Thus the addition of ferrite constituent will increase both effective ε and μ of the composite.

Table 2 – Summary of reflection and transmission losses of the polyvinyl chloride/iron-yttrium garnet composites with 0.2-30 % YIG mass concentration

Sample	Reflection loss, dB			Transmission loss, dB		
	Min.	Max.	Mean	Min.	Max.	Mean
PVC	-23.7	-21.6	-22.8	-0.14	-0.07	-0.10
0.2 %	-22.3	-20.7	-21.6	-0.20	-0.10	-0.16
0.5 %	-22.4	-20.7	-21.7	-0.20	-0.11	-0.15
1 %	-23.1	-21.3	-22.3	-0.23	-0.14	-0.19
5 %	-22.1	-20.3	-21.3	-0.17	-0.07	-0.13
10 %	-22.2	-20.4	-21.4	-0.27	-0.18	-0.23
20 %	-22.4	-20.5	-21.6	-0.30	-0.22	-0.27
30 %	-21.0	-19.3	-20.3	-0.38	-0.34	-0.34

REFERENCES

1. E.P. Wohlfarth, K.H.J. Buschow, *Ferromagnetic Materials: A Handbook of the Properties of Magnetically Ordered Substances* (Amsterdam: North-Holland: 1980).
2. S.J. Salih, W.M. Mahmood, *Heliyon* **9** No 6, e16601 (2023).
3. C. Song, W. Xu, N. Liedienov, I. Fesych, R. Kulagin,

The growth of average ε increases the impedance mismatch between composite film and waveguide which lead to the increased reflectivity but the growth of μ improves the matching and decreases reflection losses. Depending on which factor would be more dominant for each specific PVC/YIG composition, the total effect will be either increase or decrease of reflection losses. Overall, the measurements have shown that changes of the ferrite filler amount in the PVC composite within the concentration range of 0.5-30 % affect the reflection loss value rather insignificantly.

4. CONCLUSIONS

The thin films of composite materials based on ferrite as a filler and PVC as a matrix were manufactured and investigated. Films were obtained by the method of thermal pressing using pre-crushed with ball mills ferrite and dibutyl phthalate as a plasticizer.

The powder X-ray diffraction has confirmed the single-phase composition of commercial yttrium-iron garnet ferrite as well as its cubic garnet structure with high degree of crystallinity and crystal lattice parameter in agreement with reference data.

The IR Fourier spectroscopy method has revealed the characteristic bands of PVC and ferrite in the short-wave region. The presence of ferrite in the composite can affect the displacement of some characteristic bands of the polymer.

The microwave spectroscopy data measured for the composites with varying YIG mass concentration in the 8-12 GHz frequency band has shown that the samples have a negligible values of the reflection losses, which were rather uniform in the whole frequency band (with nonlinear variations as a function of ferrite filler concentration). The transmission losses were also small, around $-(0.1-0.4)$ dB, and have increased for larger YIG concentration, which was attributed to the growing contribution from the inherent magnetic losses of the ferrite material. Nevertheless, given the rather small samples' thicknesses, the transmission losses for thick specimens of the same composition are expected to be significant, especially for the composites with large amount of ferrite filler, e.g. 30 %. Thus, the composite PVC/YIG materials with high ferrite concentration can be potentially useful for the development of the radio absorbing coatings.

ACKNOWLEDGMENTS

This work has been supported in part by the Ministry of Education and Science of Ukraine: the Grant of the Ministry of Education and Science of Ukraine for the perspective development of a scientific direction "Mathematical sciences and natural sciences" at the Taras Shevchenko National University of Kyiv.

- Y. Beygelzimer, X. Zhang, Y. Han, Q. Li, B. Liu, A. Pashchenko, G. Levchenko, *Adv. Funct. Mater.* **32** No 30, 2113022 (2022).
4. J.M. Santos, J.A. daSilva-Santos, A.J.S. Silva, L. de los Santos Valladares, N.O. Moreno, *Ceram. Int.* **47**

- No 13, 18677 (2021).
5. O. Opuchovic, A. Kareiva, K. Mazeika, D. Baltrunas, *J. Magn. Magn. Mater.* **422**, 425 (2017).
 6. T. Ramesh, G.N. Rao, T. Suneetha, R.S. Shinde, V. Rajendar, S.R. Murthy, S.A. Kumar, *J. Supercond. Nov. Magn.* **31**, 1899 (2018).
 7. V.T. Hoai Huong, D.T. Thuy Nguyet, N.P. Duong, T.T. Loan, S. Soontaranon, L.D. Anh, *J. Sci. Adv. Mater. Dev.* **5**, 270 (2020).
 8. R.B. Borade, S.E. Shirsath, G. Vats, A.S. Gaikwad, S.M. Patange, S.B. Kadam, R.H. Kadam, A.B. Kadam, *Nanoscale Adv.* **1**, 403 (2019).
 9. B. Chacko, A.B. Thirumalasetty, V. Vijayakanth, M. Wuppulluri, *ACS Omega* **8**, 19367 (2023).
 10. R.S. Azis, M.M. Syazwan, N.M.M. Shahrani, A.N. Hapishah, R. Nazlan, F.M. Idris, I. Ismail, M.M.M. Zulkimi, I.R. Ibrahim, Z. Abbas, N.M. Saiden, *J. Mater. Sci.-Mater. El.* **29**, 8390 (2018).
 11. Y.J. Wu, H.P. Fu, R.Y. Hong, Y. Zheng, D.G. Wei, *J. Alloy. Compd.* **470**, 497 (2009).
 12. P.P. Vaishnav, U. Senaratne, E. Buc, R. Naik, V.M. Naik, G. Tsoi, L.E. Wenger, P. Boolchand, *J. Appl. Phys.* **99**, 702 (2006).
 13. S.H. Dewi, A. Mulyawan, Y. Sarwanto, D.S. Winatapura, W.A. Adi, *J. Rare Earth.* **41** No 4, 578 (2023).
 14. C. Cheng, Y. Liu, R. Ma, R. Fan, *Compos. Part A-Appl. S.* **155**, 106842 (2022).
 15. N.A.A. Zaini, N.I.Z. Azman, T.F.T. Hamid, A.G.E. Sutjipto, M.A. Jusoh, *Mater. Today* **51** No 2, 1426 (2022).
 16. H. Luo, Y. Lu, J. Qiu, *Carbon* **183**, 34 (2021).
 17. L.M. Grishchenko, D.O. Zhytnyk, I.P. Matushko, Yu.V. Noskov, V.A. Moiseienko, V.V. Klepko, O.Yu. Boldyrieva, Yu.A. Len, N.A. Atamas, V.A. Marianovskiy, O.V. Mischanchuk, V.V. Lisnyak, *Mol. Cryst. Liq. Cryst.* **768** No8, 139 (2024).
 18. L.M. Grishchenko, D.O. Zhytnyk, V.V. Klepko, I.P. Matushko, Y.V. Noskov, V.A. Moiseienko, V.Yu. Malyshev, O.V. Mischanchuk, A.I. Ivanisik, V.V. Lisnyak, *IEEE 42th International Conference on Electronics and Nanotechnology (ELNANO-2024)*, art. No 81, 161 (Kyiv: Igor Sikorsky Kyiv Polytechnic Institute: 2024).
 19. L.M. Grishchenko, D.O. Zhytnyk, I.P. Matushko, V.E. Diyuk, Y.V. Noskov, V.Yu. Malyshev, V.A. Moiseienko, O.Yu. Boldyrieva, V.V. Lisnyak, *Chem. Select* **9**, e202400432 (2024).
 20. L.M. Grishchenko, V.A. Moiseienko, V.E. Diyuk, O.Yu. Boldyrieva, A.V. Vakaliuk, V.Yu. Malyshev, I.P. Matushko, O.V. Mischanchuk, V.V. Lisnyak, *Appl. Nanosci.* **13**, 7203 (2023).
 21. I.P. Matushko, L.M. Grishchenko, V.A. Moiseienko, O.V. Mischanchuk, V.V. Trachevskiy, V.Yu. Malyshev, O.Yu. Boldyrieva, V.E. Diyuk, *Mol. Cryst. Liq. Cryst.* **768** No 1, 76 (2024).
 22. V.E. Diyuk, A.N. Zaderko, L.M. Grishchenko, S. Afonin, R. Mariychuk, M. Kaňuchová, V.V. Lisnyak, *Appl. Nanosci.* **12**, No 7, 2103 (2022).
 23. D.R. Bhosale, S.I. Patil, *AIP Adv.* **12**, 065103 (2022).
 24. A.A. Serga, A.V. Chumak, B. Hillebrands, *J. Phys. D: Appl. Phys.* **43**, No26, 264002 (2010).
 25. S. Tan, W. Zhang, L. Yang, J. Chen, Z. Wang, *J. Appl. Phys.* **128** No18, 183904 (2020).

Мікрохвильові поглинальні властивості композитного матеріалу на основі полівінілхлориду та ітрієвого гранату

Л.М. Гріщенко¹, Д.О. Житник², М.О. Попов², Г.Л. Чумак², В.Ю. Малишев², І.В. Фесич²,
Ю.В. Носков³, А.І. Іванісік², І.П. Матушко²

¹ Інститут хімії поверхні ім. О.О. Чуйка, Національна академія наук України, 03164 Київ, Україна

² Київський національний університет імені Тараса Шевченка, 01601 Київ, Україна

³ Інститут біоорганічної хімії та нафтохімії ім. В.П. Кухаря, Національна академія наук України, 02160 Київ, Україна

У цьому дослідженні повідомляється про виготовлення гнучких полівінілхлоридних композитних плівок із вбудованим залізо-ітрієвим гранатом та аналіз їх мікрохвильових властивостей. Плівки товщиною 0,25 мм створювали за допомогою температурного пресування при 175 °C і 10 МПа з конденсацією наповнювача залізо-ітрієвого гранату від 0,2 до 30 мас. % та дибутилфталату, як пластифікатора. Як феритовий порошок, так і виготовлені плівки були охарактеризовані за допомогою СЕМ, ТГА, ПРСА та Фур'є-ІЧС. Аналіз SEM показав, що феритовий порошок $\text{Y}_3\text{Fe}_5\text{O}_{12}$ складається з агломерованих, майже сферичних кристалітів. EDX-аналіз підтвердив наявність лише ітрію, заліза та кисню, що свідчить про високу чистоту зразка. Термогравіметричний аналіз продемонстрував високу термостабільність фериту $\text{Y}_3\text{Fe}_5\text{O}_{12}$, втрата маси складала лише 1,42 % при нагріванні від 25 до 900 °C. За даними дифракційного експерименту встановлено, що досліджуваний зразок є однофазним і має високий ступінь кристалічності. З ІЧ-спектру фериту ітрію $\text{Y}_3\text{Fe}_5\text{O}_{12}$ встановлено, що в діапазоні 550–680 cm^{-1} спостерігаються три інтенсивні смуги поглинання при 566 cm^{-1} , 610 cm^{-1} і 656 cm^{-1} , характерні для асиметричних валентних коливань Fe-O тетраедричної групи FeO_4 . Аналіз спектрів плівок показує присутність ПВХ і фериту завдяки їх чітким характерним спектральним смугам. Встановлено, що присутність фериту в композиті може викликати зміщення деяких характерних для полімера смуг. Мікрохвильові вимірювання виявили дуже низькі втрати на проходження – (0,1-0,3) дБ і незначне відбиття. Втрати на відбиття були в діапазоні від –19,3 до –23,7 дБ, демонструючи нерівномірну зміну від концентрації фериту: втрати спочатку зростали зі збільшенням вмісту фериту, потім зменшувалися, а потім знову збільшувалися.

Ключові слова: Залізо-ітрієвий гранат, Полівінілхлорид, Композитний матеріал, Мікрохвильові втрати; Електромагнітне екранування; Матеріали, що поглинають мікрохвилі.